

pubs.acs.org/Macromolecules Article

## TIRP—Thiol-Induced, Light-Activated Controlled Radical **Polymerization**

Lorand Bonda, Daniel J. Valles, Tillmann L. Wigger, Jan Meisner, Adam B. Braunschweig, and Laura Hartmann\*

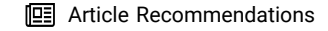


Cite This: Macromolecules 2023, 56, 5512-5523



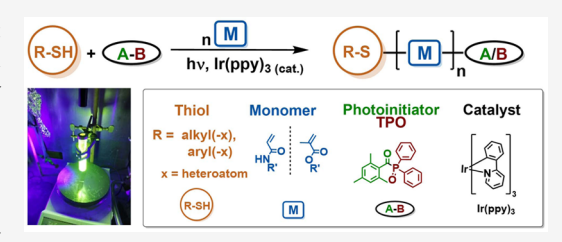
**ACCESS** I

Metrics & More



Supporting Information

ABSTRACT: Controlled radical polymerizations (CRPs) are one of the most important ways to obtain uniform, defined molecular weight polymers with complex composition and architecture such as block copolymers. A new controlled and light-initiated radical polymerization is introduced that makes use of thiol initiators and an Ir-photocatalyst. Different reaction parameters are studied for their importance in the controlled characteristics of polymerization, such as low dispersity, control of molecular weights, and straightforward access to block copolymers. The light control furthermore allows for simple switching on and off of the polymerization. We propose a mechanism for the so-called



thiol-induced, light-activated, controlled radical polymerization (TIRP), which includes the formation of dormant species and their light- and catalyst-dependent equilibrium with the active polymer chain end. TIRP enriches the portfolio of controlled and lightinitiated polymerization methods by its viability at mild conditions and the possibility to grow polymers from a large variety of readily available thiols.

#### ■ INTRODUCTION

Free radical polymerization (FRP) is typically associated with the easy and fast synthesis of polymers and compatibility with a large variety of monomers and reaction conditions. 1,2 In comparison to the ionic polymerizations, however, control over chain lengths, end groups, dispersity, and access to block copolymers is limited.<sup>3</sup> Combining the advantages of free radical and ionic polymerizations, reversible deactivation radical polymerizations (RDRPs) or in short CRPs were developed.4 The most prominent representatives are atom transfer radical polymerization (ATRP),5 reversible additionfragmentation chain-transfer polymerization (RAFT)<sup>6,7</sup> and nitroxide-mediated radical polymerization (NMP).8 The common denominator of these methods is the equilibrium between an active, growing, and a deactivated, sleeping (or dormant) form of the polymer chain end. By pushing the equilibrium to the side of the dormant species, termination reactions are drastically reduced. This results in narrow average molecular weight distributions, low dispersities, and control over end groups. Typically, these controlled polymerizations are thermally activated. In the last decade, there has been a great interest in developing alternative activation options, such as redox-controlled, 10 enzymatic, 11 high voltage, 12 or directly activated polymerizations. <sup>13</sup> Of the emerging activation methods, photoactivated <sup>14–17</sup> controlled radical polymerization (photo-CRP)<sup>18</sup> is of particular interest because light is accessible, low-cost, low-energy, is environmentally benign compared to other activators, and polymer propagation can easily be controlled by simply turning the light on and off. 19,20

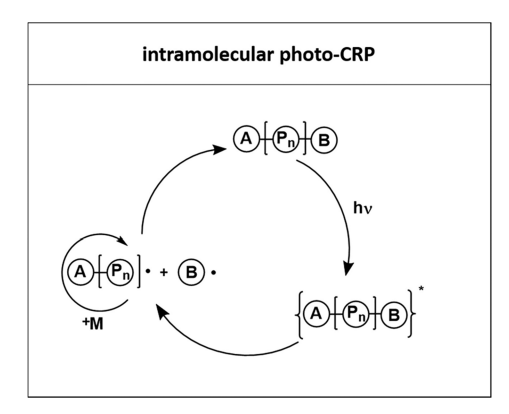
Both metal-catalyzed and metal-free photo-CRPs<sup>21</sup> have been developed and demonstrated for their use in various applications. 4,22 In general, photo-CRPs occur in two different variants, the intramolecular reaction and the photoredox reaction<sup>23,24</sup> (Figure 1). In the intramolecular reaction, light irradiation cleaves the photoactive, dormant species, releasing the active chain end for polymerization. An example of intramolecular photo-CRPs is the UV-mediated RAFTpolymerization  $^{1\hat{6,25,26}}$  which, compared to the thermally activated RAFT, uses special transfer reagents that can be activated through UV light. In the photoredox variant of CRPs, a photocatalyst is added, which generates a propagating radical by excitation with light. Two examples of photoredox CRPs are the photo-ATRP18,27,28 and the photo electron transfer RAFT (PET-RAFT).<sup>29</sup> In photo-ATRP,<sup>27</sup> an air-stable copper(II) halide is reduced by light to the copper(I) species, then mediating the ATRP. Hawker et al.<sup>30</sup> presented a way to perform photo-ATRP by using tris(2-phenylpyridine)iridium-(III)  $(Ir(ppy)_3)$  as a photocatalyst.

Recently, Wong et al.<sup>31</sup> introduced a photoinduced thiolacrylate polymerization (photo-TAP) exclusively used so far for grafting polymers onto solid surfaces. The polymerization

Received: April 26, 2023 Revised: May 25, 2023 Published: July 6, 2023







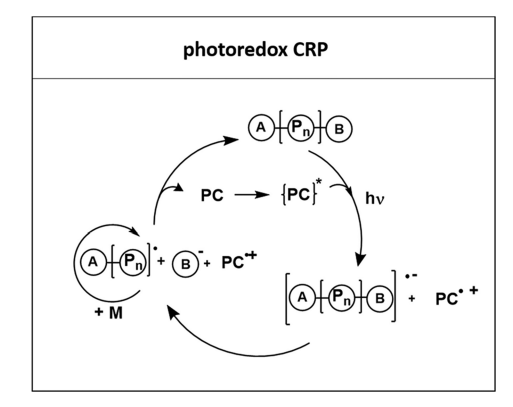


Figure 1. General mechanism of intramolecular photo-CRPs (left) and photoredox CRPs (right).<sup>23</sup>

was carried out on thiol-modified glass, and tert-butyl methacrylate (tBMA) was used as the monomer. With a photoinitiator/catalyst system consisting of diphenyl-(2,4,6trimethylbenzoyl)-phosphine oxide (TPO) and Ir(ppy)3, highly uniform polymer brush patterns (e.g., in terms of the height and positioning of polymers at the surface) were obtained. TPO is a known and widely used photoinitiator for light-activated FRP. Ir(ppy)<sub>3</sub> is a photocatalyst, <sup>32,33</sup> which is used in single electron transfer (SET) reactions, e.g., photo-ATRP<sup>19,30</sup> or PET-RAFT,<sup>29</sup> and is often used as a photoredox catalyst. The controlled surface-initiated thiol-(meth)acrylate polymerization (SI-TAP<sup>31</sup>) was carried out by irradiation with UV-light at 405 nm wavelength. By varying the TPO- and Ir(ppy)<sub>3</sub>-concentration, a linear relationship of the resulting polymer brush height with increasing amounts of TPO or Ir(ppy)3 was found. In addition, it was shown that growth on the surface was linear only up to a certain irradiance intensity (852  $\mu$ W/cm<sup>2</sup>). If this value was exceeded, polymer growth was no longer uniform. Another interesting aspect is the control of polymer growth by switching the light source on and off. If the irradiation was interrupted, the polymer growth stagnated. When the light source was switched on again, polymer growth started anew. Thus photo-TAP shows typical features of a CRP, however, this could not be further investigated as the process has been restricted to surface polymerizations. In this work, we therefore investigate this polymerization in solution. To highlight that this is a new method going beyond SI-TAP, e.g., in terms of the variety of applicable thiol initiators, analysis of molecular weights and dispersities of derived polymers, reinitiation, and accessibility of block copolymers and compatibility with other in-solution methods, we now call this thiol-induced, light-activated controlled radical polymerization (TIRP). We aim at demonstrating the controlled radical mechanism and the synthetic possibilities of TIRP, thereby adding another reaction to the small group of very impactful controlled polymerization reactions and one that is initiated from simple and widely available thiols.

#### **■ EXPERIMENTAL SECTION**

**Materials.** Chemical compounds that were not synthesized were obtained from commercial sources and used without further purification. Acetonitrile (99.9%, HPLC-grade), hydrochloric acid 1 M (p.a.), diethyl ether (p.a.), dichloromethane (99.9%, puriss., p.a.), D-(+)-mannose (99%), 2-methyl-2-propanethiol (99%), (3-nitrobenzyl)-mercaptane (97%), sodium chloride (98%), thiophenol (97%), 2-(trimethylsilyl)ethanethiol (95%), and triphenylmethanethiol (97%) were purchased from Sigma-Aldrich. Dichloromethane

(p.a.), dimethylformamide (98%, for peptide synthesis), and ethyl acetate (analytical reagent grade) were purchased from ACROS Organics. Methanol (p.a.), acetic anhydride (99.7%), and pyridine were purchased from VWR Chemicals. Tris(2-phenylpyridine)-iridium(III) (99%) was purchased from BLDpharm. Diphenyl-(2,4,6-trimethylbenzoyl)-phosphine oxide (>98%) and N-hydroxyethylacrylamide (>98%) were purchased from TCI chemicals.

**Methods.** *UV-Light Source.* Samples were irradiated with a UV-LED Spot P standard (405 nm) from Opsytec Dr. Gröbel GmbH. *Irradiation Intensities.* Irradiation intensities were determined with a FieldMaxII-TO Laser Power Meter from Coherent.

Nuclear Magnetic Resonance.  $^1$ H NMR spectra were recorded at room temperature with a Bruker AVANCE III 300 (for 300 MHz) and 600 (for 600 MHz).  $^{31}$ P NMR spectra were recorded at room temperature with a Bruker AVANCE III 300. The chemical shifts were reported relative to solvent peaks (chloroform and water) as internal standards and reported as  $\delta$  in parts per million (ppm). Multiplicities were abbreviated as s for singlet, d for doublet, t for triplet, and m for multiplet.

Matrix-Assisted Laser Desorption-Ionization Time of Flight (MALDI-TOF). MALDI-TOF spectra were recorded with a MALDI-TOF Ultraflex I provided by Bruker Daltonics. The sinapinic acid matrix applied in a mixture of acetonitrile and water (ratio of 1:2) was selected

Size Exclusion Chromatography—Multi-Angle Light Scattering ( $H_2O$ -SEC-MALS). SEC analysis was conducted with an Agilent 1200 series HPLC system and three aqueous SEC columns provided by Polymer Standards Service (PSS). The columns were two Suprema Lux analytical columns (8 mm diameter and 5  $\mu$ m particle size) and one precolumn (50 mm, 2 × 160 Å of 300 mm and 1000 Å of 300 mm). The eluent was a buffer system consisting of MilliQ water and 30% acetonitrile with 50 mM, NaH<sub>2</sub>PO<sub>4</sub>, 150 mM NaCl, and 250 ppm NaN<sub>3</sub> with a pH = 7.0 (via addition of 50 mL of 3 molar aqueous sodium hydroxide solution) filtered with an inline 0.1  $\mu$ m membrane filter and running at 0.8 mL per min. Multi-angle light scattering is recorded via miniDAWN TREOS and differential refractive index spectra with Optilab rEX both supplied by Wyatt Technologies EU. Data analysis was committed with Astra 5 software and a dn/dc value of 0.156 for each polymer.

Tetrahydrofuran-Śize Exclusion Chromatography (THF-SEC). THF-SEC measurements were carried out with a Viscotek VE 3580 RI detector and a SYKAM S 3250 UV/Vis detector equipped with a polystyrene column (300  $\times$  8.0 mm, 5  $\mu$ m) and a polyacryl column (300  $\times$  8.0 mm, 5  $\mu$ m). A S5200 (SYKAM) sample injector as an auto sampler was utilized. THF was used as a solvent and toluene as a reference. The measurements were carried out with an injection volume of 100  $\mu$ L and a flow rate of 1 mL/min. The molecular weights were determined with the Chromatographica (hs GmbH) software.

SEC (Center of Macromolecular Structure Analysis at the Leibniz Institute of Polymer Research in Dresden). SEC analysis was conducted with an Agilent 1260 series HPLC system, one precolumn, and three aqueous SEC columns provided by GE Healthcare. The

columns were three Suprema Lux analytical columns (100/100/1000). The eluent was a buffer system consisting of MilliQ water with 10 mM PBS buffer with pH = 7.4 and running at 1 mL per min. Multi-angle light scattering is recorded via DAWN Heleos-II (Wyatt),  $\lambda$  = 660 nm, and differential refractive index spectra with Optilab TrEX (Wyatt),  $\lambda$  = 660 nm, both supplied by Wyatt Technologies EU. Data analysis was committed with Astra software and a dn/dc value of 0.163 for each polymer.

Freeze Dryer. Lyophilization was performed with an Alpha 1-4 LD instrument provided by Martin Christ Freeze Dryers GmbH. A temperature of -42 °C and a pressure of 0.1 mbar were maintained throughout the freeze-drying process.

Elemental Analysis. The ratios of carbon, hydrogen, nitrogen, and sulfur were determined using a Vario Micro Cube provided by Analysensysteme GmbH. The measurements were carried out by the Institute for Pharmaceutical and Medicinal Chemistry, Heinrich-Heine University Düsseldorf.

High-Pressure Liquid Chromatography (HPLC). RP-HPLC/MS (Reversed Phase-HPLC/Mass Spectroscopy) was performed on an Agilent Technologies 1260 Infinity System using an AT 1260 G4225A degasser, G1312B binary pump, G1329B automatic liquid sampler, G1316C thermostatted column compartment, G1314F variable wavelength detector at 214 nm, and an AT 6120 quadrupole containing an electrospray ionization (ESI) source. The mobile phase consisted of buffer C (water-acetonitrile 95:5 (v/v), 0.1 vol % formic acid) and buffer D (water-acetonitrile 5:95 (v/v), 0.1 vol % formic acid). HPLC runs were performed on a Poroshell 120 EC-C18 (3.0  $\times$ 50 mm, 2.5  $\mu$ m) RP column from Agilent at a flow rate of 0.4 mL/ min 95% buffer A and 5% buffer B (0-5 min), following a linear gradient to 100% buffer B (5-30 min) at 25 °C. ESI-MS for GlcNAcoligomers and sulfates was performed using 95% buffer A and 5% buffer B without formic acid and a fragmentor voltage of 40-60 V (m/z range of 200-2000).

Computational Details. For the optimization of minimum structures and transition states, the B3LYP<sup>34</sup> functional was employed with the def2-TZVP<sup>35</sup> basis set. Electronic energies and gradients were calculated using Turbomole<sup>36</sup> version 7.2.1 with an accuracy of 10<sup>-9</sup> atomic units and the multigrid m5. To account for dispersion, the D3 dispersion correction<sup>37</sup> with Becke-Johnson damping<sup>38</sup> was used. Stationary points have been validated in their nature by the correct number of negative eigenvalues of the corresponding Hessian matrices: zero for minima and one for transition states. Geometry optimizations were performed using the DL-FIND<sup>39</sup> optimization library interfaced to Turbomole via Chemshell.<sup>40</sup> Solvation effects were accounted by using the COSMO<sup>41</sup> implicit solvation model  $(\varepsilon_{\rm DMF} = 37.51)^{42}$  For the calculation of free energies, a modified rigid-rotor-harmonic-oscillator approximation was used: frequencies below 100 cm<sup>-1</sup> have been set to this value to avoid divergence of the entropic term.

**Synthesis.** General Procedure of TIRP. One equivalent of Nhydroxyethylacrylamide monomer (HEAA, 100 mol %) or tert-butyl methacrylamide (TBMA, 100%) and tris(2-phenylpyridine)iridium-(III)  $(Ir(ppy)_3, z \text{ mol}\%)$  are dissolved in DMF [10 wt %] sealed in a 5 mL glass flask and flushed with argon as inert gas for 10 min. In a second step, the thiol compound (x mol%) and equimolar amounts of diphenyl-(2,4,6-trimethylbenzoyl)-phosphine oxide (TPO, y mol% = x mol%) are also dissolved in DMF [10 wt %] and sealed in a 5 mL microwave reaction vial. A spatula tip of TCEP is dissolved in a single drop of H<sub>2</sub>O and added to the reaction solution to reduce possible disulfides. The thiol/TPO solution is flushed under an Ar-atmosphere for 10 min and irradiated with UV-light (405 nm wavelength, intensity dependent on thiol and monomer used) for 3 min. Subsequently, the monomer/Ir(ppy)<sub>3</sub> mixture is added to the TPO/thiol solution under an inert atmosphere, and the polymerization solution is irradiated further at an unchanged light intensity. After an hour, the irradiation is stopped and the polymer solution precipitated in diethyl ether (PHEAA) or H<sub>2</sub>O/MeOH 1:3 (v/v) (PTBMA). The precipitated PHEAA is dissolved in H2O, dialyzed against distilled water (three cycles, exclusion size-dependent on molecular weight), and subsequently lyophilized.

PHEAA-block-PHEAA. HEAA monomer (500 mg, 4.3 mmol) (1 eq) and  $Ir(ppy)_3$  (0.05 mol %) are dissolved in DMF [10 wt %] sealed in a 5 mL glass flask and flushed with argon gas for 10 min. In a second step, the macro initiator polymer (55 mg, 0.0275 mmol) is also dissolved in DMF [10 wt %] and sealed in a 5 mL microwave reaction vial. A spatula tip of TCEP is dissolved in a single drop of  $H_2O$  and added to the reaction solution to reduce possible disulfides. After the monomer/ $Ir(ppy)_3$  mixture is added to the vial (inert atmosphere), the solution is irradiated with UV-light (405 nm wavelength, with an intensity of 45.2 mW/cm² (100%)). After an hour, the irradiation is stopped and the polymer solution is precipitated in diethyl ether. The precipitated polymer is dissolved in  $H_2O$ , dialyzed against distilled water (three cycles, 10 kDa), and subsequently lyophilized.

PHEAA-block-PManAAm. AcO-ManAAm (966.6 mg, 2.17 mmol, see SI chapter 2.2 for synthesis) (1 eq) and Ir(ppy)<sub>3</sub> (0.05 mol %) are dissolved in DMF [10 wt %] sealed in a 5 mL glass flask and flushed with argon gas for 10 min. In a second step, the macro initiator polymer (0.6 g, 0.086 mmol) is also dissolved in DMF [10 wt %] and sealed in a 5 mL microwave reaction vial. A spatula tip of TCEP is dissolved in a single drop of H2O and added to the reaction solution to reduce possible disulfides. After the monomer/Ir(ppy)3 mixture is added to the vial (inert atmosphere), the solution is irradiated with UV light (405 nm wavelength, with an intensity of 45.2 mW/cm<sup>2</sup> (100%)). After an hour, the irradiation is stopped and 5 mL of NaOMe (0.2 M) in MeOH was added to the polymer solution and stirred one hour at room temperature. The sample solution is precipitated in diethyl ether. The precipitated polymer is dissolved in H<sub>2</sub>O, dialyzed against distilled water (three cycles, 5 kDa), and subsequently lyophilized.

#### ■ RESULTS AND DISCUSSION

Controlled Features of TIRP—Dispersity and Reinitiation. To determine if TIRP has the key features of a controlled radical polymerization (low dispersity, controllable molecular weights, linear correlation between degree of polymerization (DP) and monomer conversion, reinitiation), a first set of reactions was carried out using commercially available acrylamide (*N*-hydroxyethylacrylamide (HEAA)) and methacrylate (*tert*-butyl methacrylate) monomers, the photo-initiator/catalyst system consisting of TPO as the initiator and Ir(ppy)<sub>3</sub> as the catalyst, and tritylthiol as the thiol component, as it is easy to handle and can be easily detected in <sup>1</sup>H NMR-spectroscopy (Scheme 1). The thiol/TPO ratio was set to 1:1,

Scheme 1. TIRP in Solution (Polymerizations #1 and #2)

and the amount of thiol—TPO was increased from 1 mol % in the first polymerization to 5 mol % in the second polymerization to achieve different chain lengths at a similar overall monomer concentration [1.7 mmol] (Table 1). Molecular weights and dispersity of the obtained poly(N-hydroxyethylacrylamide) (PHEAA) were determined by aqueous size exclusion chromatography-multiangle light scattering (SEC-MALS) coupled with an RI detector, showing that both polymers are obtained with much lower dispersity (D = 1.09 - 1.10, additional data via RI-MALS, see SI chapter 2) than is expected for an FRP (see the SI for control reaction performed as FRP by leaving out the thiol initiator giving D = 1.7 at DP of

Table 1. Thiol-TPO Ratios with Average Molecular Weights and Dispersities Obtained for #1, #2, #1', and #2'

#	thiol conc. [mol %]	TPO conc. [mol %]	irradiation intensity $\left[mW/cm^2\right]$	$\bar{M}_{\rm n}~[{ m kDa}]^a$ theoretical (via SEC)	$\overline{P}_{\mathrm{n}}$ theoretical (calculated)	$\mathcal{D}^a$ via SEC
1	1	1	2.61	11.8 (12)	100 (98)	1.1
2	5	5	2.61	2.7 (2.7)	20 (20)	1.09
1'	1	1	1.15	14.2 (14.6)	100 (103)	1.3
2′	5	5	1.15	2.8 (2.7)	20 (18)	1.3

"Via SEC-MALS-RI (precolumn (50 mm, 2 × 160 Å of 300 mm and 1000 Å of 300 mm), two main columns (8 mm diameter and 5  $\mu$ m particle size), eluent: MilliQ water—acetonitrile 7:3 ( $\nu/\nu$ ), 50 mM, NaH<sub>2</sub>PO<sub>4</sub>, 150 mM NaCl and 250 ppm NaN<sub>3</sub>, pH = 7.0, flow rate: 0.8 mL/min; for additional measurements with SEC-MALS-RI detector, see SI, chapter 2.

70).<sup>43</sup> The same is found for poly(*tert*-butyl methacrylate) (PTBMA) dispersities determined by THF-SEC, with RI and UV detectors ( $\mathcal{D} = 1.0-1.4$ ). Molecular weights for both polymers closely match the theoretically expected molecular weights (Table 1).

To further demonstrate the potentially living character of TIRP, kinetic measurements were recorded during the polymerization of HEAA with tritylthiol as the thiol source. A characteristic of controlled polymerizations is a linear relation between chain growth and conversion, in contrast to the exponential relation in FRPs. Samples were taken from the polymerization solution at defined times and the conversion was determined by <sup>1</sup>H NMR spectroscopy (see SI, chapter 2.1.3 for details). As shown in Figure 2A, reaction time is

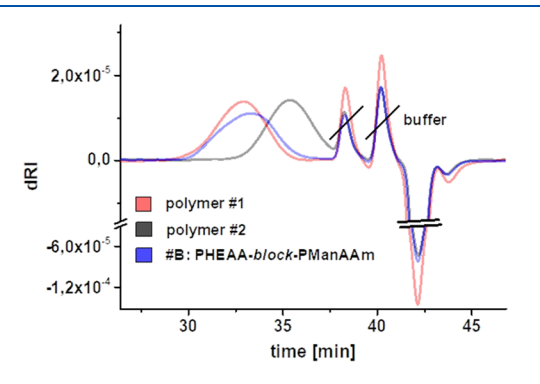


**Figure 2.** Aqueous SEC-MALS measurement of polymer #1, polymer #2 (Scheme 1), and PHEAA-block-PManAAm (Scheme 2B, copolymer #B).

plotted against the monomer conversion, showing a curve previously reported also for other light-activated CRPs such as PET-RAFT. Maximum conversion is reached after 60 min for a polymer of 2.7 kDa ( $\overline{P}_n = 20$ ) (#2) and after 90 min for a polymer of 14.2 kDa ( $\overline{P}_n = 100$ ) (#1). We observed that conversion reaches a plateau at around 70%. At this time, we attribute this to deactivation of the catalyst, as has previously been shown for other CRP systems, e.g., ATRP. Alternatively, a complete deactivation of the growing chains is highly unlikely, as this would have resulted in much higher dispersities than observed. It is also known that the polymerization of acrylamide monomers with full conversions is challenging in commonly used CRPs such as ATRP. However, this phenomenon will be investigated further in future experiments.

Figure 3B shows the plot of  $\ln([M]_0/[M]_t)$  against the reaction time (with  $[M]_0$  = initial monomer concentration and  $[M]_t$  = monomer concentration at reaction time t). An ideal living polymerization is expected to give a linear correlation in such a plot. <sup>47</sup> For TIRP, we observe a nearly linear correlation with a light tilt downward at higher reaction times. This has

also been observed for other CRPs and indicates termination events likely by recombination and disproportionation that can occur from the radical chain ends. For example, Driessen et al. 47 showed such tilting for well-established ATRP reactions.

One of the interesting features of light-controlled polymerizations is the ability to stop polymerization by switching the light source off as well as to (re-)start the reaction again when turning the light source back on. To test whether this occurs in the TIRP, the polymerization was performed by switching repeatedly the light off and then back on again, and conversion was determined before and after each on/off cycle by <sup>1</sup>H NMR spectroscopy. We observed stagnation of the conversion during "light off" periods, with continuing conversion when the light is switched on again (Figure 3C).

The control over polymer growth by switching the light source on and off (Figure 3C), as well as the linear relationship of conversion and degree of polymerization (Figure 3D) show typical characteristics of light-controlled polymerizations. The evolution of molecular weight, respectively, the degree of polymerization was observed via  $^1{\rm H}$  NMR spectroscopy. SEC analysis was not suitable here as especially for the lower  $\overline{P}_{\rm n}$  samples, polymers could not be isolated from the reaction mixture without discriminating against parts of the sample (e.g., shorter chains).

The possibility of growth control through switching the light source on/off and comparison to other controlled systems also suggests that a dormant species is present which can be reinitiated. Thus, next, we tested whether it is possible to reinitiate, not only in the reaction solution itself but also from a polymer that is first isolated by precipitation and then used in a second, independent polymerization to derive a block copolymer (Scheme 2). Therefore, further HEAA (#A) and tetra-acetylated mannose-acrylamide monomer (AcO-ManA-Am, #B, see SI, chapter 2.2 for synthesis of the monomer) were used as comonomers for two separate reinitiation reactions.

Employing the previous TIRP conditions (thiol/TPO ratio 1:1, 6 mol % each, 0.05 mol % Ir(ppy)3, based on 1 eq of monomer), the PHEAA precursor of 2 kDa was purified and isolated by precipitation, dialysis, and freeze-drying. This precursor was reinitiated with the same monomer by addition of HEAA and Ir(ppy)<sub>3</sub>, while not introducing any additional thiol/TPO. Molecular weight analysis by aqueous SEC-MALS shows an increase in the number averaged molecular weight  $(\overline{M}_n)$  from 2 to 20 kDa. Dispersity for the elongated polymer increases from 1.1 to 1.3 (Scheme 2). In a second experiment, AcO-ManAAm was used to prepare a block copolymer. Here, a PHEAA precursor of 7 kDa was again purified and isolated as described above and then reinitiated by the addition of ManAAm and Ir(ppy)<sub>3</sub>. The resulting PHEAA-block-PManAAm (#B) was analyzed by <sup>1</sup>H NMR, showing distinct signals of both blocks, as well as by SEC-MALS, giving a mean molecular weight  $(M_n)$  of 13.5 kDa and a dispersity of 1.2 (see

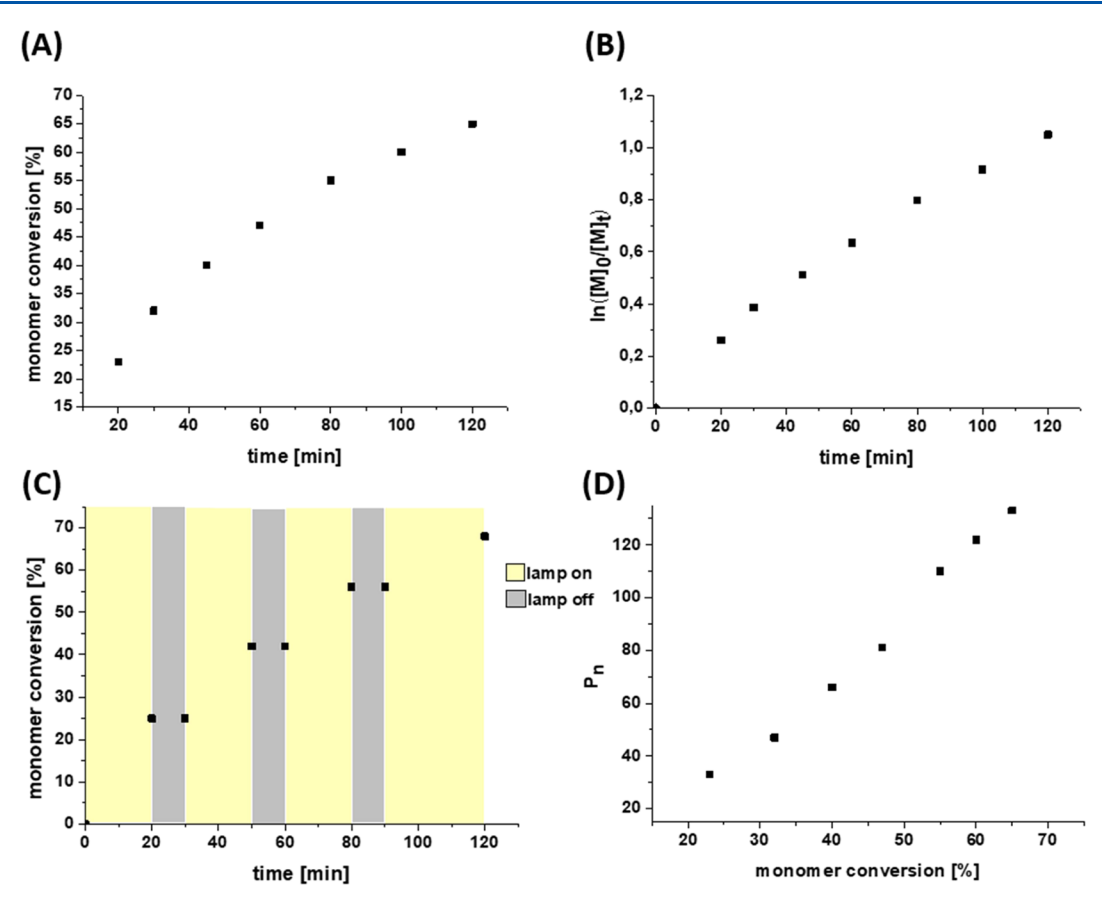


**Figure 3.** (A) Monomer conversion (determined by  ${}^{1}H$  NMR spectroscopy) versus reaction time (#1); (B) logarithmic plot of  $M_{0}/M_{t}$  ( $M_{0}$  = initial monomer concentration,  $M_{t}$  = monomer concentration at reaction time (t) against reaction time (#1); (C) monomer conversion (determined by  ${}^{1}H$  NMR spectroscopy) versus irradiation time while light is switched on/off (#1); (D) degree of polymerization against monomer conversion [%] (determined via  ${}^{1}H$  NMR spectroscopy by referencing the tritylthiol initiator protons; for further information, see SI, chapter 2.1.5).

# Scheme 2. (A) Elongation of PHEAA through Reinitiation (Copolymer #A) and (B) Copolymerization with AcO-ManAAm (Copolymer #B)

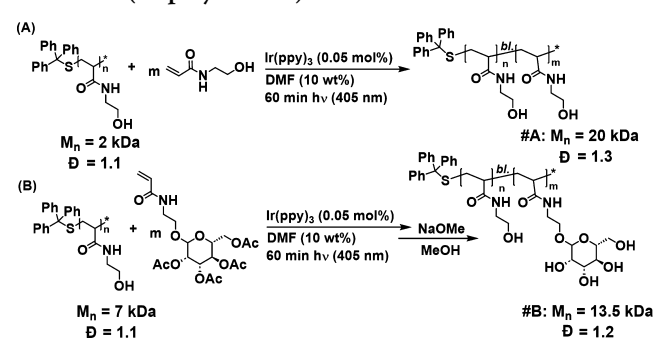
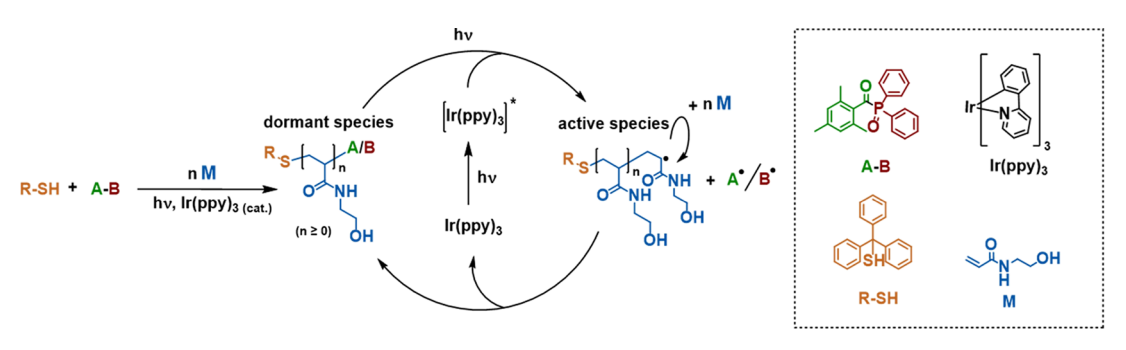


Figure 2). Thus, polymers prepared by TIRP can be reinitiated to obtain block copolymers, which is another important feature of CRPs.

For comparison, free radical copolymerization was performed by synthesis of a precursor PTBMA ( $\overline{M}_n=7.7~\mathrm{kDa}$ ) with the use of a TPO initiator but no thiol source. This FRP generates a polymer bearing TPO fragments as end groups. After isolation, the precursor polymer was reinitiated without addition of any further initiator (TPO; thiol) but ethyl acrylate as a comonomer (synthesis of precursor and copolymer, see SI, chapter 2.2.2). The resulting copolymer shows an increase in  $\overline{M}_n$  (9.5 kDa), evidencing successful reinitiation. The dispersities of both polymers (precursor and copolymer, D=2) are higher than those obtained by TIRP (D=1.2-1.3) and

Scheme 3. Potential Mechanism for the Initiation and Chain Growth Reaction in TIRP via Intramolecular Photo-CRP



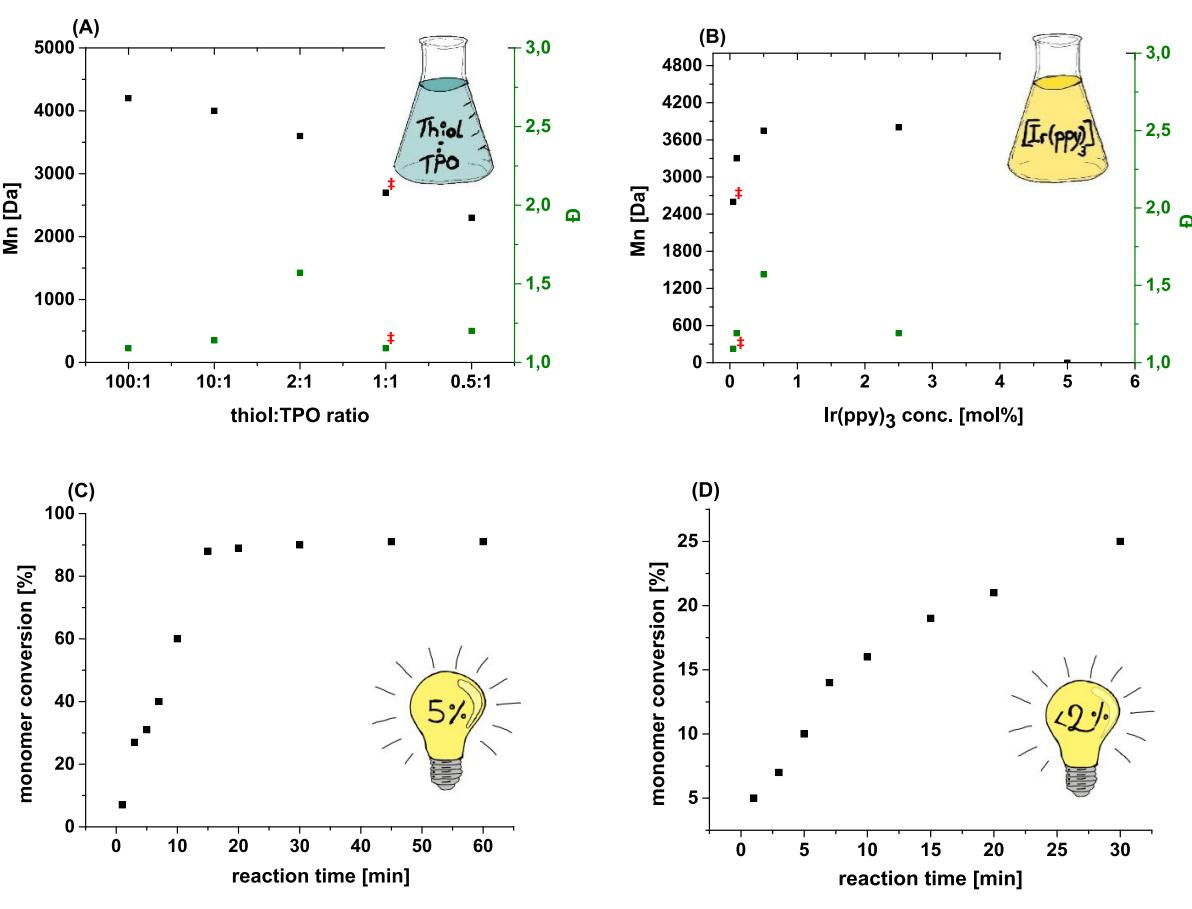


Figure 4. (A) Average molecular weights and dispersities obtained by changing thiol—TPO;  $\overline{M}_n$  theory: 2700 Da;  $^{\ddagger}$ highlighted data point shows optimized TIRP reaction conditions with thiol—TPO ratio 1:1,  $[Ir(ppy)_3] = 0.05 \text{ mol } \%$ ,  $h\nu$  intensity = 5%; (B) average molecular weights and dispersities obtained by varying  $[Ir(ppy)_3]$ ;  $\overline{M}_n$  theory: 2700 Da;  $^{\ddagger}$ highlighted data point shows optimized TIRP reaction conditions with  $[Ir(ppy)_3] = 0.05 \text{ mol } \%$ , thiol—TPO ratio 1:1,  $h\nu$  intensity = 5%; (C) kinetic studies using 2-(trimethylsilyl)-ethanethiol as a thiol source at 5% irradiation intensity; (D) kinetic studies using 2-(trimethylsilyl)-ethanethiol as a thiol source at <2% irradiation intensity.

are characteristic for FRPs. Thus, this experiment shows that reinitiation of polymers bearing TPO-fragments as the end group is possible, supporting our proposed mechanism (Scheme 3). However, these polymers lack the control over the chain length and dispersity obtained by TIRP. To the best of our knowledge, the reinitiation and synthesis of block-coplymers from FRP by using TPO as the initiator have also not been demonstrated before and thus are another important findings of this study. Future studies will follow up on this methodology, while here, the focus is on demonstrating the controlled features and opportunities of TIRP.

Parameters of TIRP. Next, we explored the mechanism of TIRP by studying the effects of the different reaction conditions and components on the resulting polymers. If not stated otherwise, HEAA was used as the monomer and tritylthiol as the thiol component. All reactions were performed in DMF as the solvent, at room temperature, and with 405 nm UV-light because both, TPO and Ir(ppy)<sub>3</sub>, absorb at this wavelength. 48,16

**Thiol-TPO Ratio.** Our first hypothesis on the potential mechanism assumes that TPO forms radicals by photocleavage that then abstract a proton from the thiol compound, giving a thiyl radical that will start the polymerization reaction. Ideally, only the thiyl radical starts the polymer chain by reacting with a first monomer. TPO, as a photoactive radical initiator, is capable of starting polymerizations as well, forming what we call TPO-polymers in contrast to the targeted TIRP products

that polymerize from the thiyl radical. If the thiol source is omitted, polymers are formed but have high dispersity, indicating that TPO-polymers are formed by FRP (see SI, chapter 2.2.2). When using a 1:1 ratio of thiol/TPO, as we have done in the first polymerization reactions (#1 and #2, Scheme 2), we observed the following features that are characteristic of controlled polymerizations: linear kinetics, low dispersity, and molecular weights that match the theoretically expected chain length. When the concentration of TPO is lower than the concentration of thiol, we observed higher molecular weights than would have expected based on the thiol-monomer ratio (Figure 4A). This suggests that only a fraction of possible thiol initiators is activated, thereby reducing the number of growing chains. If more TPO than thiol is used, all thiols are activated, but also extra TPO remains, which can initiate additional polymer chains. As a result, molecular weights are decreased and dispersity is increased (see SI, chapter 2.3). Thus, the optimal ratio of TPO-thiol to achieve controlled TIRP is equimolar (1:1) (see Scheme 1).

**Ir(ppy)**<sub>3</sub>. To obtain TIRP with the characteristics of a CRP, the use of the photocatalyst Ir(ppy)<sub>3</sub> is mandatory. If no Ircatalyst is used, polymers are formed but have high dispersity and do not show sulfur in the elemental analysis (see SI, Figure S49). Both results indicate that only TPO-polymers are formed. These results also suggest that the thiol source does not undergo unwanted chain transfer reactions, which are

typical for thiols in FRPs.<sup>49</sup> If transfers occur, the resulting dispersities would be expected to be higher than those observed. Furthermore, higher sulfur content would have been expected to be measured in the elemental analysis but was not found (see SI, chapter 2.5.1). In addition, the reaction is sensitive to the amount of Ir-catalyst: If too high of an amount of Ir(ppy)3 is used (>2.5 mol % based on [monomer]), polymerization does not occur. When increasing Ir(ppy)<sub>3</sub> concentrations below this critical value (0-2.5 mol %), the average molecular weight increases with increasing Ir concentration (Figure 4B), but the yield drops with increasing Ir mol%. The optimum amount of Ir(ppy)<sub>3</sub> was found to be 0.05 mol % (based on [monomer]). Here, polymers with chain lengths, as determined by SEC, that are in very good agreement with the theoretically calculated chain lengths were obtained, in good yields, and with low dispersities (see SI, chapter 2.1).

*hν* **Intensity.** The irradiation intensity is one of the most important parameters when it comes to controlling the TIRP. Based on the previously established optimized reaction conditions (equimolar ratio of thiol and TPO, 0.05 mol % photocatalyst), polymerizations were performed at either 1.15 mW/cm² (2%), 2.61 mW/cm² (5%), or 45.2 mW/cm² (100%) intensity at 405 nm.

At 100% intensity, we again observe features that are associated with FRP (deviation of molecular weights from theoretical values, high dispersity). At an intensity of 2%, (HEAA as the monomer, tritylthiol as the thiol source), no polymerization occurred. When using only TPO at 2% intensity, the polymer is formed. The ideal intensity was found to be 5% (2.61 mW/cm<sup>2</sup>), where controlled polymerization characteristics were observed (see SI, chapter 2.5). To investigate this further, the reaction was carried out with a ratio thiol-TPO of 1:2. As expected, polymers are formed matching FRP characteristics (no thiol content, higher dispersity) (see SI, Table S7). To rule out potential absorption effects of the trityl group of the thiol component, the polymerization was carried out again at 2% light intensity, using triphenylmethanol or triphenylmethylchloride instead of tritylthiol at a 1:1 ratio with TPO. In both cases, polymers were obtained, indicating that the presence of phenyl substituents on the thiol group do not limit the formation of radicals from TPO fragmentation.

By varying the monomer from HEAA to TBMA (thiol—TPO 1:1,  $[Ir(ppy)_3] = 0.05 \text{ mol }\%$ ), 5% intensity already led to FRP characteristics, so irradiation intensity had to be decreased to 2% to regain controlled features. This shows that light intensity has to be adapted to the monomer which we attribute to the different reactivity in radical polymerization of the monomers (methacrylate > acrylamide). This is further supported by our finding that for *tert*-butyl acrylate (TBA), with a further increase in reactivity, at the lowest intensity setting possible with our set-up (1.15 mW/cm²), we obtained polymers with typical features of FRP only ( $\mathcal{D}=1.6-2.4$ ) (see SI, chapter 2.5.2) We assume, that for successful TIRP of acrylate monomers, intensity has to be decreased further.

**Thiol Source.** One great advantage of TIRP is the availability of a large variety of different thiols that can be selected as initiators. To understand how the structure of the thiol compounds affects the TIRP, the previously used tritylthiol was replaced by 2-(trimethylsilyl)-ethanethiol (TMS-thiol). HEAA was used as the monomer. Under the reaction conditions optimized for tritylthiol (thiol—TPO ratio 1:1, 5% irradiation intensity, 0.05 mol % Ir(ppy)<sub>3</sub>), polymers

with molecular weights close to the theoretical value ( $\overline{M}_{\rm n}$  theory = 2.7 kDa), although with high dispersity (>3), were obtained. Kinetic studies show that the molecular weight first increases exponentially as the conversion progresses but then reaches a plateau. Such exponential growth is typical for FRPs (Figure 4C). However, by further reducing the light intensity to <2%, a chain growth with a constant progress relation was observed (Figure 4D). Thus, we conclude that, as in the case for monomers, for different thiols, a different light intensity is required to realize TIRP with CRP characteristics. This is likely related to the different kinetics of initiating chain growth when using different thiol sources.

We tested a first series of different thiol derivatives and show that they all can successfully be used as initiators in TIRP (Figure 5; see SI, chapter 2.7). Each thiol, however, requires its

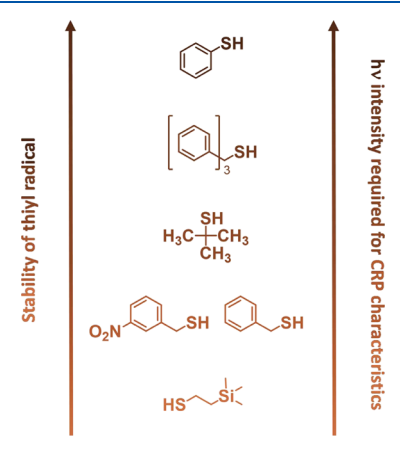


**Figure 5.** Thiols used to initiate TIRP (HEAA = 1 eq, Ir(ppy)<sub>3</sub> = 0.05 mol %, DMF = 10 wt %,  $h\nu$  = 60 min, varying intensities; 405 nm; for additional data, see SI, chapter 2.7).

own optimal irradiation intensity to keep the controlled characteristics of the polymerization. As an example, tritylthiol did not initiate polymerization at 2% irradiation intensity, but polymerization took place at 5% irradiation intensity. Thiophenol, on the other hand, showed no polymerization at 5% irradiation intensity, so the irradiation intensity was increased to 30% (see SI, Table S10).

TMS-thiol polymers were already formed at 2% irradiation intensity, but the reaction showed FRP characteristics, indicating that the intensity needs to be decreased further to regain CRP characteristics. Generally, we observed that primary thiols require less irradiation intensity than secondary or tertiary thiols. A possible explanation is that as primary thiol radicals are less stabilized than tertiary or phenylic ones, the rate-limiting step might be to initiate polymer propagation. Initiation at a more stabilized radical could require a higher light intensity, while the reaction of a primary, less-stabilized radical already occurs at a lower irradiation intensity.

Potential TIRP Mechanism. Based on our observations on the effects of the different reaction parameters and quantum chemical calculations of the different initiation and propagation steps (see SI, chapter 3), we postulate a potential mechanism for TIRP. We have seen that in the absence of thiol, upon irradiation, TPO forms two radical-bearing fragments (mesityl fragment (A) and phospine fragment (B), Scheme 3) and starts a FRP (TPO-polymers). As we have shown and discussed before, also FRP TPO-polymers can be reinitiated and give access to blockcopolymers, yet with less

**Figure 6.** Reaction of tritylthiol, TPO, and Ir(ppy)<sub>3</sub> without monomers (intermediates 1 and 2) and after adding 1 eq HEAA (intermediates 1' and 2') or *n* eq. HEAA (polymers 1" and 2") to the reaction. Determined molecular weights via RP-HPLC-MS and MALDI-ToF are shown (including the hydrolysis product DPPA, 3); for RP-HPLC-MS measurement spectra of intermediates 1, 1', 2, and 3, see SI, Figures S99 and S100. For the MALDI-ToF spectrum of polymerization performed under optimized conditions (1" and 4), see SI, Figure S95.

control over the chain length and dispersity. In the case of the CRP, in the presence of both thiol and the Ir catalyst, TPO fragment(s) first abstract a hydrogen from the thiol. The resulting thiyl radical initiates chain elongation, leading to polymers with chain ends consisting of the thiol compound, as seen in MALDI-ToF-MS (see SI, Figure \$95). For a controlled mechanism, a dormant species must form. We hypothesize that the dormant species in TIRP is formed by recombination of the active chain end (thiyl radical for n = 0) with one of the TPO fragments (A, if B abstracted the hydrogen or B, if A abstracted the hydrogen in the initiation reaction) (Figure 6). We confirm the formation of this dormant species, tritylthiol, Ir(ppy)<sub>3</sub>, and TPO was irradiated in the absence of monomers (Figure 6). RP-HPLC-MS analysis of the reaction mixture indeed confirms the formation of intermediate 2 (RS-B, see SI, Figure S100). As reported by Sluggett et al., 51 the reactivity of the two different TPO fragments in order to achieve hydrogen transfer onto a thiol is approximately equal. Therefore, we assume that also 1 (RS-A) is formed but is not detected by RP-HPLC-MS due to the detection limit. When repeating the experiment in the presence of one equivalent of monomer per TPO/thiol, polymer chains with  $\overline{P}_n = 1$  were identified by RP-HPLC-MS, with end groups consisting of the thiol as well as the TPO mesityl fragment 1' (RS-M-A, see SI, Figure S99). In all cases, an additional signal at m/z = 219 was found and is assigned as diphenylphosphinic acid (DPPA, 3, see SI, Figures S99 and S100). We assume that the second dormant species, 2' (RS-M-B), was also formed but that the TPO-end group was hydrolyzed under LC conditions (aqueous acidic conditions) releasing DPPA 3. The trityl group is also not

detected in any of the structures, as it is well known to be easily cleaved under even slightly acidic conditions. <sup>52</sup> Overall, these findings support our postulated mechanism (Scheme 3).

To confirm that the same end groups are also present in higher molecular weight polymers, end group analysis by MALDI-ToF-MS was performed. The MALDI-ToF (see SI, Figure S95) shows the end groups of a polymer synthesized with optimized TIRP conditions (thiol-TPO 1:1, 0.05 mol % Ir(ppy)<sub>3</sub>, 5% irradiation intensity) for tritylthiol and HEAA. The signals with the highest relative intensity are spaced with m/z = 115.13, which corresponds to the mass of the monomer. Dormant species, RS-M<sub>n</sub>-A (polymer 1") and RS-M<sub>n</sub>-B (polymer 2"), can be identified. In addition, chain ends formed through recombination, as known from FRP, are also found, although at lower relative intensity (see SI, Figure S98). The presence of polymers from these termination reactions is also known for other CRPs. 53,54 For comparison, MALDI-ToF end group analysis was also performed for conditions that do not follow controlled polymerization characteristics (thiol-TPO ratio not at 1:1, too high irradiation intensity for tritylthiol as well as TMS-thiol) (see SI, Figures S96 and S97). In all cases, a larger number of different end groups was observed, which were assigned to end groups from dormant species, end groups from FRPs, and mixtures thereof (TPOinitiated and recombined), as is expected for a less controlled reaction. To further confirm the phosphorus containing TPO end groups, <sup>31</sup>P NMR spectra were recorded of species 2, 2', and 2". For all three compounds, a phosphorus signal is found in the spectra (see SI, Figures S102-S104), supporting our findings from MS analysis.

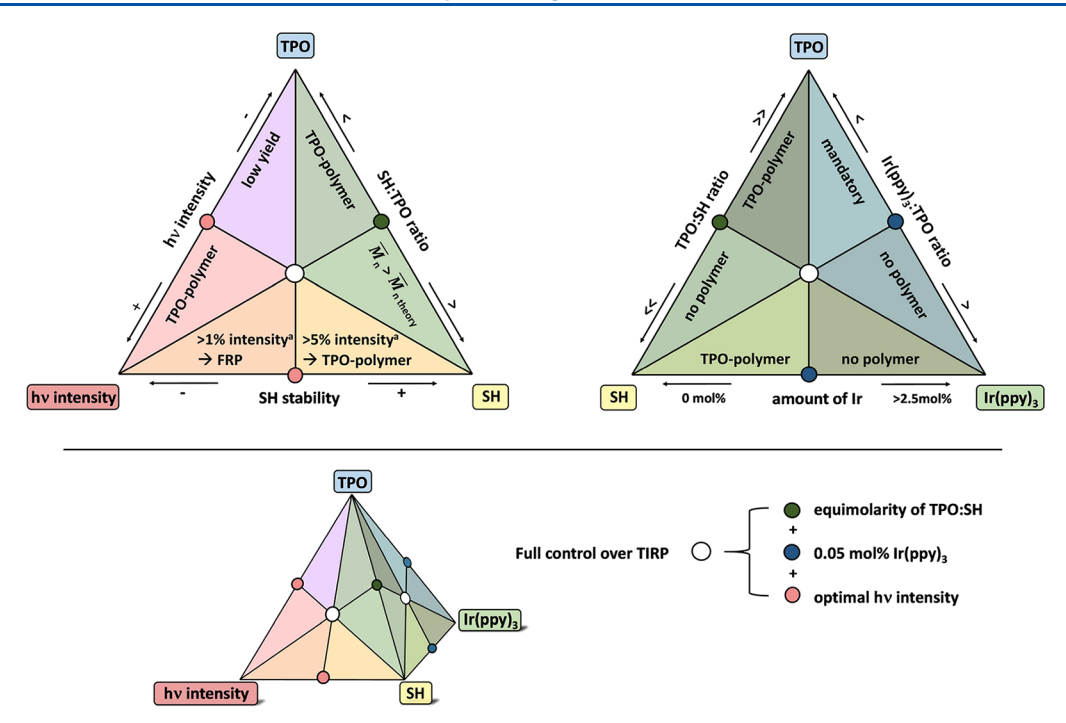


Figure 7. Triangle and tetrahedron depictions of the interrelationships and limits of TIRP when varying polymerization parameters: [a] $h\nu$  intensity (405 nm) of 2%  $\triangleq$  1.15 mW/cm<sup>2</sup>.

Thus, our studies confirm the presence of RS-M<sub>n</sub>-A species (see SI, Figure S95) and RS-M<sub>n</sub>-B (see SI, Figure S97) which, according to our postulated mechanism (Scheme 3), are the dormant species of TIRP. In order to undergo controlled polymerization, dormant species have to exist in an equilibrium with the active species, the radical chain end of the growing polymer chain. We can conclude that the photocatalyst is required as well as a light source of appropriate wavelength and intensity. This is also demonstrated by performing the polymerization in two steps: first, tritylthiol, Ir(ppy)3, and TPO were irradiated without any monomer, and formation of RS-B was confirmed by RP-HPLC-MS (see SI, Figure S100). Only upon addition of HEAA monomers and a second period of irradiation, polymers with end groups consistent with the proposed dormant species are formed (see SI, Figure S99). Interestingly, in comparison to the one-pot procedure, which is the general TIRP procedure used in this work (see SI, chapter 1), slightly higher irradiation intensity is required in the polymerization step of the two-step process, where first, the intermediates 1 and 2 are built, isolated, and used for initiation.

To further support our postulated mechanism, quantum chemical calculations of the individual mechanistic steps were performed. The barrier of an initial monomer reacting with tritylthiol is 10.7 kcal/mol and should therefore happen almost instantaneously. The free energy barriers for adding one monomer "M" to RS-M radicals was computed to be 17.7 kcal/mol (see SI, chapter 3 for further details), which is energetically feasible. We computed the free dissociation energy of RS-M<sub>n</sub>-A to be 44.5 kcal/mol and RS-M<sub>n</sub>-B 52.1 kcal/mol when following an intramolecular photo-CRP mechanism (see also Figure 1). This value is below the energy of a 405 nm photon (70.6 kcal/mol), so the dissociation of A or B from RS-M<sub>n</sub> is energetically possible. In comparison, the energy required for electron transfer from  $Ir(ppy)_3$  to RS- $M_n$ -A or RS-M<sub>n</sub>-B, which would correspond to a photoredox CRP mechanism (also see Figure 1), is 76.7 and 80.5 kcal/mol,

respectively. Therefore, we hypothesize a photocatalytic activation through an intramolecular homolytic cleavage reaction rather than a photoredox process. These computations support the postulated mechanism shown in Scheme 3.

Sweet Spot Conditions for TIRP. Taken together, our study shows that there are three rules that need to be followed to achieve TIRP with controlled characteristics: (1) a thiol—TPO ratio of 1:1 should be maintained; (2) the concentrations of  $Ir(ppy)_3$  has to be ~0.05 mol % of the overall monomer content (=100 mol %) and should not exceed 2.5 mol %; (3) the irradiation intensity needs to be optimized based on the chosen thiol initiator/monomer. Based on these parameters, a "sweet spot" for the TIRP reaction can be identified (Figure 7).

We have also seen that these parameters are interdependent. To highlight how the different reaction parameters play together in giving the "sweet spot", we have plotted a diagram (tetrahedron), as is depicted in Figure 7, showing the interrelationships that have been identified in this study. For the left triangle (Figure 7), an optimal amount of Ir(ppy)<sub>3</sub> is set, while for the right triangle, an optimum light intensity is set. Going along the sides of each triangle, we can now follow the previously described trends. For example, when more thiol than TPO is used or vice versa, noncontrolled polymerization is observed. When the light intensity is too low, no polymerization occurs. If the light intensity is too high, noncontrolled polymerization occurs. Stabilized thiyl radicals such as the tritylthiol require higher light intensities than less stabilized thiyl radicals. Increasing the amount of Ir(ppy)<sub>3</sub> increases molecular weights; however, above 2.5 mol % Ircatalyst, polymerization no longer takes place, with an optimal amount of 0.05 mol % Ir(ppy)<sub>3</sub> relative to the monomer concentration.

We can already explain some of these correlations based on our postulated mechanism. Other parameters and their correlation are not yet understood, e.g., the necessity of a

higher irradiation intensity in the two-step polymerization process. While such optimization of reaction parameters can be tedious in solution, in the future, SI-TAP and the straightforward analysis of polymer growth on the surface by measuring the height can be used for simplified screening of optimized TIRP conditions, e.g., when varying the thiol initiators.<sup>30</sup>

#### CONCLUSIONS

We demonstrate that thiol-initiated polymerizations can be performed under controlled conditions and as light-controlled polymerizations in solution when using TPO and Ir(ppy)<sub>3</sub> as the co-initiator and catalyst, as had been initially observed on surfaces. We demonstrate the use of different initiators and monomers in the synthesis of low dispersity homo- as well as block copolymers. In the future, we anticipate that TIRP will enrich the portfolio of both controlled as well as light-activated polymerization methods and can specifically make use of a variety of natural and synthetic thiols to derive complex polymer conjugates including block copolymers.

#### ASSOCIATED CONTENT

#### **Supporting Information**

The Supporting Information is available free of charge at https://pubs.acs.org/doi/10.1021/acs.macromol.3c00789.

<sup>1</sup>H NMR spectra; H<sub>2</sub>O-SEC data; THF-SEC data; ESI-MS; MALDI-ToF-MS; <sup>31</sup>P NMR spectra; reaction kinetic data; monomer synthesis; block copolymer synthesis and characterization; optimization studies; variation of polymerization parameters; and quantum chemical calculations (PDF)

#### AUTHOR INFORMATION

#### **Corresponding Author**

Laura Hartmann — Institute of Organic Chemistry and Macromolecular Chemistry, Heinrich-Heine-University Duesseldorf, Duesseldorf D-40225, Germany; Institute for Macromolecular Chemistry, University of Freiburg, Freiburg im Breisgau D-79104, Germany; orcid.org/0000-0003-0115-6405; Email: laura.hartmann@hhu.de

#### Authors

Lorand Bonda – Institute of Organic Chemistry and Macromolecular Chemistry, Heinrich-Heine-University Duesseldorf, Duesseldorf D-40225, Germany

Daniel J. Valles – Advanced Science Research Center, Graduate Center, City University of New York, New York, New York 10031, United States; PhD Programs in Chemistry and Biochemistry, Graduate Center, City University of New York, New York, New York 10016, United States

Tillmann L. Wigger – Institute for Physical Chemistry, Heinrich-Heine-University Duesseldorf, Duesseldorf D-40225, Germany

Jan Meisner — Institute for Physical Chemistry, Heinrich-Heine-University Duesseldorf, Duesseldorf D-40225, Germany; ⊚ orcid.org/0000-0002-1301-2612

Adam B. Braunschweig — Advanced Science Research Center, Graduate Center, City University of New York, New York, New York 10031, United States; PhD Programs in Chemistry and Biochemistry, Graduate Center, City University of New York, New York, New York 10016, United States; Department of Chemistry, Hunter College, New York, New

York 10065, United States; o orcid.org/0000-0003-0344-3029

Complete contact information is available at: https://pubs.acs.org/10.1021/acs.macromol.3c00789

#### **Author Contributions**

The manuscript was written through contributions of all authors. All authors have given approval to the final version of the manuscript.

#### Notes

The authors declare the following competing financial interest(s): The authors (LB,DJV,ABB and LH) have filed for a patent application based on the findings presented in the study.

#### ACKNOWLEDGMENTS

We thank Susanne Boye from the polymer separation group at the Leibniz-Insitut of Polymer Research in Dresden for her great support with the SEC measurements. Also, we thank the CeMSA@HHU (Center for Molecular and Structural Analytics @ Heinrich-Heine University) for recording the mass spectrometric and the NMR-spectroscopic data. ABB acknowledges support from the US National Science Foundation (DBI-2032176), the Air Force Office of Scientific Research (FA9550-19-1-0220 and FA9550-23-1-0230), and the Army Research Office (W911NF2010271). Computational infrastructure and support were provided by the Centre for Information and Media Technology at Heinrich-Heine University Düsseldorf. J.M. is grateful for a materials cost allowance from the Fonds der Chemischen Industrie.

#### **■** REFERENCES

- (1) Staudinger, H. A Source Book in Chemistry, 1900–1950; Harvard University Press: Cambridge, MA, 2013.
- (2) Nesvadba, P. Radical polymerization in industry. *Encycl. Radic. Chem., Biol. Mater.* **2012**, 1962–1997.
- (3) Pan, X.; Tasdelen, M. A.; Laun, J.; Junkers, T.; Yagci, Y.; Matyjaszewski, K. Photomediated controlled radical polymerization. *Prog. Polym. Sci.* **2016**, *62*, 73–125.
- (4) Destarac, M. Controlled radical polymerization: industrial stakes, obstacles and achievements. *Macromol. React. Eng.* **2010**, *4*, 165–179.
- (5) Matyjaszewski, K.; Xia, J. Atom transfer radical polymerization. *Chem. Rev.* **2001**, *101*, 2921–2990.
- (6) Chiefari, J.; Chong, Y.; Ercole, F.; Krstina, J.; Jeffery, J.; Le, T. P.; Mayadunne, R. T.; Meijs, G. F.; Moad, C. L.; Moad, G. Living free-radical polymerization by reversible addition—fragmentation chain transfer: the RAFT process. *Macromolecules* **1998**, *31*, 5559–5562.
- (7) Moad, G.; Rizzardo, E.; Thang, S. H. Living radical polymerization by the RAFT process—a third update. *Aust. J. Chem.* **2012**, *65*, 985–1076.
- (8) Hawker, C. J.; Bosman, A. W.; Harth, E. New polymer synthesis by nitroxide mediated living radical polymerizations. *Chem. Rev.* **2001**, *101*, 3661–3688.
- (9) Yeow, J.; Boyer, C. Photoinitiated Polymerization-Induced Self-Assembly (Photo-PISA): New Insights and Opportunities. *Adv. Sci.* **2017**, *4*, No. 1700137.
- (10) Chen, C. Redox-controlled polymerization and copolymerization. *ACS Catal.* **2018**, *8*, 5506–5514.
- (11) Zhang, B.; Wang, X.; Zhu, A.; Ma, K.; Lv, Y.; Wang, X.; An, Z. Enzyme-initiated reversible addition—fragmentation chain transfer polymerization. *Macromolecules* **2015**, 48, 7792—7802.
- (12) Magenau, A. J. D.; Strandwitz, N. C.; Gennaro, A.; Matyjaszewski, K. Electrochemically Mediated Atom Transfer Radical Polymerization. *Science* **2011**, 332, 81–84.

- (13) McKenzie, T. G.; Fu, Q.; Uchiyama, M.; Satoh, K.; Xu, J.; Boyer, C.; Kamigaito, M.; Qiao, G. G. Beyond traditional RAFT: alternative activation of thiocarbonylthio compounds for controlled polymerization. *Adv. Sci.* **2016**, *3*, No. 1500394.
- (14) Yagci, Y.; Jockusch, S.; Turro, N. J. Photoinitiated polymerization: advances, challenges, and opportunities. *Macromolecules* **2010**, 43, 6245–6260.
- (15) Bian, S.; Zieba, S. B.; Morris, W.; Han, X.; Richter, D. C.; Brown, K. A.; Mirkin, C. A.; Braunschweig, A. B. Beam pen lithography as a new tool for spatially controlled photochemistry, and its utilization in the synthesis of multivalent glycan arrays. *Chem. Sci.* **2014**, *5*, 2023–2030.
- (16) Chapman, R.; Jung, K.; Boyer, C. Photo RAFT Polymerization. RAFT Polymerization: Methods, Synthesis and Applications; 2021; vol 1, pp 611–645.
- (17) Valles, D. J.; Zholdassov, Y. S.; Braunschweig, A. B. Evolution and applications of polymer brush hypersurface photolithography. *Polym. Chem.* **2021**, *12*, 5724–5746.
- (18) Carbonell, C.; Valles, D.; Wong, A. M.; Carlini, A. S.; Touve, M. A.; Korpanty, J.; Gianneschi, N. C.; Braunschweig, A. B. Polymer brush hypersurface photolithography. *Nat. Commun.* **2020**, *11*, 1244.
- (19) Dolinski, N. D.; Page, Z. A.; Discekici, E. H.; Meis, D.; Lee, I. H.; Jones, G. R.; Whitfield, R.; Pan, X.; McCarthy, B. G.; Shanmugam, S.; Kottisch, V.; Fors, B. P.; Boyer, C.; Miyake, G. M.; Matyjaszewski, K.; Haddleton, D. M.; de Alaniz, J. R.; Anastasaki, A.; Hawker, C. J. What happens in the dark? Assessing the temporal control of photomediated controlled radical polymerizations. *J. Polym. Sci., Part A: Polym. Chem.* **2019**, *57*, 268–273.
- (20) Aydogan, C.; Yilmaz, G.; Shegiwal, A.; Haddleton, D. M.; Yagci, Y. Photoinduced Controlled/Living Polymerizations. *Angew. Chem., Int. Ed.* **2022**, No. e202117377.
- (21) Junkers, T.; Laun, J. Controlled reversible deactivation radical photopolymerization. In *Photopolymerisation Initiating Systems*; The Royal Society of Chemistry: Cambridge, 2018; pp 244–273.
- (22) Bagheri, A.; Jin, J. Photopolymerization in 3D printing. ACS Appl. Polym. Mater. 2019, 1, 593-611.
- (23) Prier, C. K.; Rankic, D. A.; MacMillan, D. W. Visible light photoredox catalysis with transition metal complexes: applications in organic synthesis. *Chem. Rev.* **2013**, *113*, 5322–5363.
- (24) Chen, M.; Zhong, M.; Johnson, J. A. Light-controlled radical polymerization: mechanisms, methods, and applications. *Chem. Rev.* **2016**, *116*, 10167–10211.
- (25) Quinn, J. F.; Barner, L.; Barner-Kowollik, C.; Rizzardo, E.; Davis, T. P. Reversible addition—fragmentation chain transfer polymerization initiated with ultraviolet radiation. *Macromolecules* **2002**, *35*, 7620–7627.
- (26) Otsu, T.; Matsunaga, T.; Doi, T.; Matsumoto, A. Features of living radical polymerization of vinyl monomers in homogeneous system using N, N-diethyldithiocarbamate derivatives as photo-iniferters. *Eur. Polym. J.* **1995**, *31*, 67–78.
- (27) Tasdelen, M. A.; Uygun, M.; Yagci, Y. Photoinduced controlled radical polymerization. *Macromol. Rapid Commun.* **2011**, *32*, 58–62.
- (28) Dadashi-Silab, S.; Atilla Tasdelen, M.; Yagci, Y. Photoinitiated atom transfer radical polymerization: Current status and future perspectives. *J. Polym. Sci., Part A: Polym. Chem.* **2014**, *52*, 2878–2888.
- (29) Xu, J.; Jung, K.; Atme, A.; Shanmugam, S.; Boyer, C. A robust and versatile photoinduced living polymerization of conjugated and unconjugated monomers and its oxygen tolerance. *J. Am. Chem. Soc.* **2014**, *136*, 5508–5519.
- (30) Fors, B. P.; Hawker, C. J. Control of a living radical polymerization of methacrylates by light. *Angew. Chem., Int. Ed.* **2012**, *124*, 8980–8983.
- (31) Wong, A. M.; Valles, D. J.; Carbonell, C.; Chambers, C. L.; Rozenfeld, A. Y.; Aldasooky, R. W.; Braunschweig, A. B. Controlledheight brush polymer patterns via surface-initiated thiol-methacrylate photopolymerizations. *ACS Macro Lett.* **2019**, *8*, 1474–1478.
- (32) Lalevée, J.; Blanchard, N.; Tehfe, M. A.; Peter, M.; Morlet-Savary, F.; Fouassier, J. P. A novel photopolymerization initiating

- system based on an iridium complex photocatalyst. *Macromol. Rapid Commun.* **2011**, 32, 917–920.
- (33) Lee, C.-L.; Lee, K. B.; Kim, J.-J. Polymer phosphorescent light-emitting devices doped with tris (2-phenylpyridine) iridium as a triplet emitter. *Appl. Phys. Lett.* **2000**, *77*, 2280–2282.
- (34) Becke, A. D. A new mixing of Hartree–Fock and local density-functional theories. *J. Chem. Phys.* **1993**, *98*, 1372–1377.
- (35) Schäfer, A.; Huber, C.; Ahlrichs, R. Fully optimized contracted Gaussian basis sets of triple zeta valence quality for atoms Li to Kr. *J. Chem. Phys.* **1994**, *100*, 5829–5835.
- (36) Ahlrichs, R.; Bär, M.; Häser, M.; Horn, H.; Kölmel, C. Electronic structure calculations on workstation computers: The program system turbomole. *Chem. Phys. Lett.* **1989**, *162*, 165–169.
- (37) Grimme, S.; Antony, J.; Ehrlich, S.; Krieg, H. A consistent and accurate ab initio parametrization of density functional dispersion correction (DFT-D) for the 94 elements H-Pu. *J. Chem. Phys.* **2010**, 132, 154104.
- (38) Grimme, S.; Ehrlich, S.; Goerigk, L. Effect of the damping function in dispersion corrected density functional theory. *J. Comput. Chem.* **2011**, 32, 1456–1465.
- (39) Kästner, J.; Carr, J. M.; Keal, T. W.; Thiel, W.; Wander, A.; Sherwood, P. DL-FIND: an open-source geometry optimizer for atomistic simulations. *J. Phys. Chem. A* **2009**, *113*, 11856–11865.
- (40) Metz, S.; Kästner, J.; Sokol, A. A.; Keal, T. W.; Sherwood, P. Chem Shell a modular software package for QM/MM simulations. Wiley Interdiscip. Rev.: Comput. Mol. Sci. 2014, 4, 101–110.
- (41) Klamt, A. The COSMO and COSMO-RS solvation models. Wiley Interdiscip. Rev.: Comput. Mol. Sci. 2018, 8, No. e1338.
- (42) Corradini, F.; Marcheselli, L.; Tassi, L.; Tosi, G. Static dielectric constants of the N, N-dimethylformamide/2-methoxyethanol solvent system at various temperatures. *Can. J. Chem.* **1992**, *70*, 2895–2899.
- (43) Matyjaszewski, K.; Davis, T. P. Handbook of radical polymerization; Wiley Online Library, 2002, p 922.
- (44) Teodorescu, M.; Matyjaszewski, K. Controlled polymerization of (meth)acrylamides by atom transfer radical polymerization. *Macromol. Rapid Commun.* **2000**, *21*, 190–194.
- (45) Jones, G. R.; Li, Z.; Anastasaki, A.; Lloyd, D. J.; Wilson, P.; Zhang, Q.; Haddleton, D. M. Rapid synthesis of well-defined polyacrylamide by aqueous Cu (0)-mediated reversible-deactivation radical polymerization. *Macromolecules* **2016**, *49*, 483–489.
- (46) Chmielarz, P.; Park, S.; Simakova, A.; Matyjaszewski, K. Electrochemically mediated ATRP of acrylamides in water. *Polymer* **2015**, *60*, 302–307.
- (47) Driessen, F. Functional and amphiphilic copolymers by means of copper-mediated polymerization. PhD Thesis, Universiteit Gent, Polymer Chemistry Research Group, 2017.
- (48) Holzer, W.; Penzkofer, A.; Tsuboi, T. Absorption and emission spectroscopic characterization of Ir(ppy)<sub>3</sub>. *Chem. Phys.* **2005**, 308, 93–102
- (49) Cramer, N. B.; Reddy, S. K.; O'Brien, A. K.; Bowman, C. N. Thiol— ene photopolymerization mechanism and rate limiting step changes for various vinyl functional group chemistries. *Macromolecules* **2003**, *36*, 7964–7969.
- (50) Kucharski, M.; Lubczak, R. Copolymerization of hydroxyalkyl methacrylates with acrylamide and methacrylamide I. Determination of reactivity ratios. *J. Appl. Polym. Sci.* **1997**, *64*, 1259–1265.
- (51) Sluggett, G. W.; Turro, C.; George, M. W.; Koptyug, I. V.; Turro, N. J. (2, 4, 6-Trimethylbenzoyl) diphenylphosphine oxide photochemistry. A direct time-resolved spectroscopic study of both radical fragments. *J. Am. Chem. Soc.* 1995, 117, 5148–5153.
- (52) Pathak, A. K.; Pathak, V.; Seitz, L. E.; Tiwari, K. N.; Akhtar, M. S.; Reynolds, R. C. A facile method for deprotection of trityl ethers using column chromatography. *Tetrahedron Lett.* **2001**, *42*, 7755–7757
- (53) Patten, T. E.; Xia, J.; Abernathy, T.; Matyjaszewski, K. Polymers with very low polydispersities from atom transfer radical polymerization. *Science* **1996**, *272*, 866–868.
- (54) Tsujii, Y.; Ejaz, M.; Sato, K.; Goto, A.; Fukuda, T. Mechanism and kinetics of RAFT-mediated graft polymerization of styrene on a

solid surface. 1. Experimental evidence of surface radical migration. *Macromolecules* **2001**, *34*, 8872–8878.

### **□** Recommended by ACS

Light-Driven Organocatalyzed Controlled Radical Polymerization from Sulfonyl Chloride Initiators Promoted by Bis(thiocarbonyl) Disulfides

Lu Zhang, Mao Chen, et al.

JULY 21, 2023 MACROMOLECULES

READ 🗹

Fully Oxygen-Tolerant Visible-Light-Induced ATRP of Acrylates in Water: Toward Synthesis of Protein-Polymer Hybrids

Kriti Kapil, Krzysztof Matyjaszewski, et al.

FEBRUARY 20, 2023 MACROMOLECULES

READ 🗹

Reversed Controlled Polymerization (RCP): Depolymerization from Well-Defined Polymers to Monomers

Glen R. Jones, Athina Anastasaki, et al.

MAY 01, 2023

JOURNAL OF THE AMERICAN CHEMICAL SOCIETY

READ 🗹

Photoinduced 3D Printing through a Combination of Cationic and Radical RAFT Polymerization

Bowen Zhao, Jian Zhu, et al.

AUGUST 03, 2022

MACROMOLECULES

READ 🗹

Get More Suggestions >